Condensation of Water Vapor in Rarefaction Waves: II. Heterogeneous Nucleation

S. Kotake* and I. I. Glass†
Institute for Aerospace Studies, University of Toronto, Canada

A macroscopic model of heterogeneous nucleation is used for a theoretical study of condensation of water-vapor/carrier-gas mixtures in a nonequilibrium nonstationary rarefaction wave generated in a shock tube. The results are compared with those from homogeneous nucleation. It is assumed that nucleation takes place heterogeneously on idealized smooth, spherical solid particles of Aitken nuclei, which are chemically and electrically inert. In the processes of heterogeneous condensation, the controlling factors are the size-distribution of nuclei, the concentration of monomers on the surface of the substrate and the activation energy of nucleation, which is greatly dominated by the contact angle of embryos. Of these factors, the most dominant is the contact angle. Due to the reduced activation energy, heterogeneous condensation results in less supercooling of the mixture and a faster approach to the equilibrium state. By choosing a suitable value for the contact angle, the numerical results can be made to fit some recent experimental data. Although this is not entirely satisfactory, it is probably preferable to changing the value of surface tension, which was done in the homogeneous-nucleation model in order to obtain agreement with the same experimental results.

Introduction

PROBLEMS of two-phase and two-component systems have great practical importance in various engineering fields. Research into nucleation and growth by condensation and evaporation of droplets has been conducted over a long period of time and many aspects can be regarded as understood.

Homogeneous nucleation and condensation have been studied theoretically and experimentally by a number of investigators within the framework of one- or two-dimensional supersonic-nozzle flows and nonstationary rarefaction flows in a shock tube. Recently, Sislian and Glass[1] made a detailed numerical study of homogeneous nucleation and condensation of water vapor with or without a carrier gas in the nonstationary rarefaction wave generated in a shock tube and predicted the effects of condensation on the flow variables.

Unless a supersaturated vapor is specially and expensively treated, it is likely to contain a large number of small particles (Aitken nuclei), which can act as heterogeneous nuclei. Depending upon the cooling rate and the number of nuclei, the resulting phase change of the supersaturated vapor can take place at considerably lower supersaturation than predicted by homogeneous nucleation alone. The nucleation rate will depend on the nature of the surface of the nucleus, including its geometry and physical and chemical properties. It also depends on the condition of the surface and the state of the vapor.

In the present paper, by using a macroscopic model of heterogeneous nucleation,[2,3] numerical studies were made of the condensation of water vapor in a nonstationary rarefaction wave generated in a shock tube, and the results were compared with those obtained from homogeneous nucleation.[1] Nucleation was assumed to take place heterogeneously on idealized, smooth, spherical particles of Aitken nuclei, which are chemically and electrically inert.

Heterogeneous Nucleation and Condensation

Condensation Nuclei

Atmospheric air is widely used as a source of commercial nitrogen gas. The air has sufficient quantities of nuclei produced by physical, chemical, and mechanical processes in nature. According to cloud-physics terminology,[4] these particles are classified by dimension as Aitken nuclei for particles with radii below 0.1 μ; large nuclei for those with radii 0.1 ~ 1 μ; and gigantic or giant nuclei for those with radii in excess of 1 μ. Even cleaned air with careful filtration might carry a considerable number of these condensation nuclei, especially Aitken nuclei. In industrial processes, the gases are further treated by various pieces of equipment such as heat exchangers, condensers, spray-columns, contact apparatus, and filters. The number density of particles and their physical and chemical properties therefore depend not only on those in the initial gas but also on the gas-flow process. By taking special care of physical filtration and electrical neutralization, large and gigantic particles and electrically charged particles can be excluded from the gas. Consequently, the processed gas can be assumed to contain only Aitken nuclei that are chemically and electrically inert.

Concentration and size-distribution of atmospheric nuclei vary greatly with locality. A representation of the average

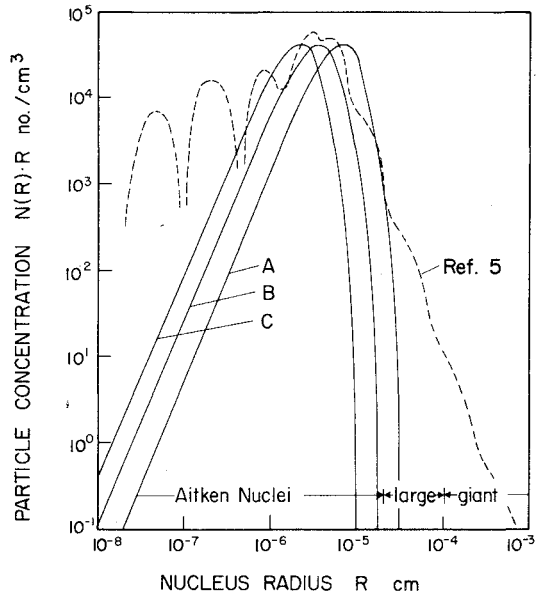

Fig. 1 Size distribution of particles.

Received June 21, 1976; revision received Oct. 20, 1976.
Index categories: Multiphase Flows; Nozzle and Channel Flow; Shock Waves and Detonations.

*Visiting Professor, 1975-76, Institute of Space and Aeronautical Science, The University of Tokyo, Tokyo, Japan.

†Professor. Fellow AIAA.

size-distribution in typical atmospheric air is shown in Fig. 1.[5] Two peaks below 3×10^{-6} cm are due to more aggregations of air and water molecules on ions and are not foreign particles. Hence, the gas treated with physical filtration and electrical neutralization can be assumed to have such a size distribution of nuclei given by curves A, B, and C. By introducing a distribution function $N(R)$, having units of cm^{-4}, with respect to the droplet radius R that the number lying in the size range from R to $R+dR$ is given by $N(R)dR$, the assumed distribution curves in Fig. 1 can be expressed as

$$\frac{dN}{d\ln R}=N(R)\cdot R=N_0\left(\frac{R}{R_0}\right)^{2.5}\exp\left\{-\left(\frac{R}{R_0}\right)^{1.5}\right\} \tag{1}$$

where $N_0=1.0\times10^{-5}$ cm^{-3}, $R_0=1.5$(A), 2.5(B), 5.0(C)$\times10^{-6}$ cm.

Particles with a radius less than 10^{-6} cm are highly dispersed and in vigorous Brownian motion so that the shape of the particles is not at all spherical due to coagulation and sintering phenomena. It may, however, be possible to classify them by some effective particle size, such as average radius. All particles are assumed to have a smooth, spherical shape of effective radius R without any further coagulation or separation.

The chemical and physical properties of Aitken nuclei are extremely varied because their formation is due not only to a number of originating processes but also to subsequent coalescence of particles, adsorption of gases, and chemical reactions. Hence, one may actually have reference only to average properties of particles. If the nuclei consist of a mixture of soluble and insoluble particles, then nucleation is dominated by the soluble particles due to their smaller activation energy. However, the gases treated with physical and chemical processes can contain only a negligible quantity of soluble particles. Here, all condensation nuclei are assumed to be chemically inert and insoluble in water vapor.

Heterogeneous Nucleation

According to the macroscopic theory[3,6] heterogeneous nucleation takes place as a result of growth beyond a critical size of embryos from a thermodynamic equilibrium distribution colliding with monomers or higher-order clusters. Consider monomers or higher-order clusters of a supersaturated vapor impinging on a surface of a solid particle R, to make a cap-shaped embryo r, as illustrated in Fig. 2. There are two types of monomer impingements on embryos; the direct impingement of monomers from the vapor[6] and the impingement by desorption of adsorbed monomers.[7] For both cases, the nucleation rate per unit surface area of nucleus particle per unit time can be expressed as[6,7]

$$\dot{n}=Z\cdot a_v^*\frac{\alpha_a}{\nu}\left(\frac{p_v}{\sqrt{2\pi mkT}}\right)^2\exp\left(-\frac{\Delta G^*-\Delta G_d}{kT}\right) \tag{2}$$

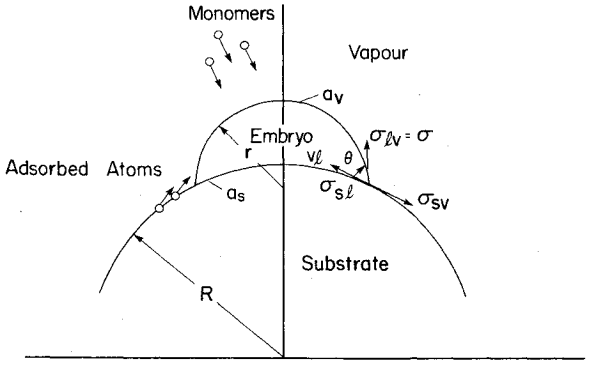

Fig. 2 Cap-shaped embryos nucleating on surface of insoluble substrate.

where ΔG^* is the Gibbs free energy of formation of an embryo, ΔG_d the desorption free energy of monomers, p_v the vapor pressure, T the temperature, m the mass of the one molecule, k the Boltzmann constant, ν the vibrational frequency of the adsorbed atom, α_a the adsorption coefficient, a^*_v the liquid-vapor interface area of the embryo, and Z the nonequilibrium correction factor. For a cap-shaped embryo, the factor Z is given by[6]

$$Z=\{\Delta G^*/(3\pi kTi^*)\}^{1/2}$$

where i^* is the number of monomers in the critical embryo.

The free energy of embryo formation is expressed as the sum of contributions from the formation of the solid-liquid interface, the liquid-vapor interface, and the bulk, being a function of the free-energy difference from vapor to liquid phase and the surface free energy of the interfaces. Differentiating this free energy of embryo formation with respect to the radius of embryo gives the critical free energy ΔG^* and the critical radius r^*

$$\Delta G^*=\frac{16\pi\sigma^3}{3(n_\ell kT\ln s)^2}\mathrm{f}\left(\frac{r^*}{R},\cos\theta\right),\quad r^*=\frac{2\sigma}{n_\ell kT\ln s} \tag{3}$$

where σ is the surface tension of liquid-vapor interface, θ the contact angle, n_ℓ the number of molecules per unit volume of liquid, s the supersaturation ($s=p_v/p_s$, p_s is the saturation pressure of the vapor), and the factor $\mathrm{f}(r/R,\cos\theta)$ is given by[8]

$$\mathrm{f}\left(\frac{r}{R},\cos\theta\right)=\frac{1}{2}\left[1+\left\{c_\theta\left(\frac{r}{R}-\cos\theta\right)\right\}^3+\left(\frac{R}{r}\right)^3\left\{2-3c_\theta\left(1-\frac{r}{R}\cos\theta\right)+c_\theta^3\left(1-\frac{r}{R}\cos\theta\right)^3\right\}+3\left(\frac{R}{r}\right)^2\cos\theta\left\{c_\theta\left(1-\frac{r}{R}\cos\theta\right)-1\right\}\right]$$

$$c_\theta\equiv\left\{1+\left(\frac{r}{R}\right)^2-2\frac{r}{R}\cos\theta\right\}^{-1/2}$$

By combining Eqs. (2) and (3), the heterogeneous nucleation rate per unit area of nucleus substrate can be expressed as

$$\dot{n}=\dot{n}_0R_H\frac{b_s}{\sqrt{f}}\sqrt{\frac{T}{T_0}}\exp\left\{\beta_d\left(\frac{T_0}{T}-1\right)\right\}\exp\left\{-\frac{4\pi}{3}\frac{r^{*2}\sigma}{kT}(f-1)\right\} \tag{4}$$

where b_s is the geometrical factor of the liquid-vapor surface of an embryo ($a_v^*/4\pi r^{*2}$) and

$$R_H=\frac{1}{\nu}\sqrt{\frac{kT_0}{2\pi m}}\,e^{\beta_d}\quad\beta_d=\frac{\Delta G_d}{kT_0}$$

with T_0 as a reference temperature of the system, namely, the temperature in the driver section, and $\dot{n}_0$ is the homogeneous nucleation rate per unit volume of vapor

$$\dot{n}_0\equiv4\pi r^{*2}\frac{p_v}{\sqrt{2\pi mkT}}\frac{p_v}{kT}\exp\left(-\frac{4\pi}{3}\frac{r^{*2}\sigma}{kT}\right) \tag{5}$$

The factors R_H and β_d are the vibrational frequency of adatoms and the desorption free energy of monomers, respectively. The values of $\nu(R_H)$ and $\Delta G_d(\beta_d)$ are somewhat uncertain and depend largely on the nucleation situation, but fortunately they are not significant quantities. For nucleus

particles of radius $\sim 10^{-5}$ cm, ΔG_d is of one or two orders smaller than ΔG^* and the exponent term of β_d therefore does not have an appreciable effect on the overall nucleation rate.

Condensation and Droplet Growth

A nucleus particle has a surface area A_0 at the initial stage of nucleation. The area is then wetted by condensed droplets at time t and the wetted area is denoted by $A_w(t)$. The nucleation rate per unit volume of vapor in the range of nuclei from R to $R+dR$ is $\dot{n}[A_0-A_w(t)]N(R)dR$, and the mass of embryos is $\rho_\ell v_\ell \dot{n}[A_0-A_w(t)]N(R)dR$ where ρ_ℓ and v_ℓ are the embryo density and volume, respectively. Considering the growth of these embryos by condensation yields the following expression of the overall condensate mass production per unit time per unit mass of vapor mixture g

$$\frac{dg}{dt}=\frac{\dot{n}_0}{\rho}\frac{4}{3}\pi r_0^{*3}\rho_\ell+\int_0^t\frac{\dot{n}_0}{\rho}\frac{d}{dt}\left(\frac{4}{3}\pi r_0^3\rho_\ell\right)d\tau$$
$$+\int_0^\infty\left[\frac{\dot{n}}{\rho}\{A_0-A_w(t)\}\frac{4}{3}\pi r^{*3}a^*\rho_\ell\right.$$
$$\left.+\int_0^t\frac{\dot{n}}{\rho}\{A_0-A_w(\tau)\}\frac{\partial}{\partial t}\left(\frac{4}{3}\pi r^3 a\rho_\ell\right)d\tau\right]N(R)dR \quad (6)$$

where ρ is the density of vapor mixture, r_0 the embryo radius for homogeneous nucleation; a the geometrical factor of the embryo volume ($v_\ell=4/3\pi r^3 a$), and the superscript * denotes the initiation stage of nucleation. The first and second terms of the right-hand side are the contributions from homogeneous nucleation. When the heterogeneous nuclei are in the size range of one or two orders greater than that of embryos ($R\sim 10^{-5}$ cm) and the contact angles are not too large ($\theta<120°$), the homogeneous nucleation rate is one or two orders smaller than the heterogeneous nucleation rate under the presently considered changes in the state variables, especially the cooling rate taken as $\lesssim 0.1°\Phi/\mu$sec. At higher cooling rates ($\gtrsim 1°C/\mu$sec) conditions become favorable for homogeneous nucleation. Therefore, homogeneous nucleation can be neglected in the present rate equation.

The wetted surface area A_s is given by

$$A_s=\int_0^t\dot{n}(\tau)\{A_0-A_w(\tau)\}a_s(t,\tau)d\tau \quad (7)$$

where $a_s(t,\tau)$ is the liquid-solid interfacial area of a condensed droplet formed at time τ. By using the Hertz-Knudsen equation for the net mass flow of vapor molecules condensing onto a droplet,[3] the droplet-growth rate can be approximately expressed as

$$\dot{r}=\frac{b_v}{a}\left(1+\frac{1}{3}\frac{r}{a}\frac{\partial a}{\partial r}\right)\dot{r}_0=K\dot{r}_0 \quad (8)$$

where b_v is the geometrical factor of the liquid-vapor interfacial area $a_v=4\pi r^2 b_v$, and $\dot{r}_0$ the growth rate for the homogeneous case

$$\dot{r}_0=\frac{\alpha}{\rho_\ell}\frac{p_s}{\sqrt{2\pi mkT}}(s-1)$$

where α is the condensation coefficient.

The integral equations (6) and (7) can be solved numerically more readily by transforming them into successive differential equations.[9] From a preliminary computation of a typical system of heterogeneous nucleation and condensation,[9] it was found that the size distribution of nuclei *A*, *B*, *C* in Fig. 1 had little influence on the results, because they have almost the same number of nuclei with a larger radius compared with embryos. It was also established that the features of heterogeneous condensation are dominated largely by the contact angle.

Governing Equations of the System

A mixture of water vapor and air or an inert carrier gas, which contains solid particles acting as heterogeneous nuclei, is initially at rest in the high-pressure driver section of a shock tube. At time $t=0$, the diaphragm separating the driver section from the low-pressure-channel section of the shock tube is suddenly ruptured, and the mixture is expanded into the channel. When sufficient supersaturation occurs, embryos of water droplets nucleate heterogeneously on the substrate of solid particles and then grow to larger water droplets by condensation of water vapor. Concerning the gasdynamic and thermodynamic features of this system, the following assumptions are made: a) the effects of molecular transport are neglected; b) solid particles move at the same speed as the mixture regardless of water-vapor condensation on them, c) the thermodynamic properties of the mixture are the weighted sums of the corresponding properties for the single system.

The gasdynamic equations coupled with the rate equation under these assumptions were solved numerically by Sislian using the method of characteristics.[10] However, as stated in Ref. 10, this method is not effective for flows when the characteristics intersect to form shock waves. In the present case of heterogeneous nucleation it is assumed that the same features prevail, namely, that the condensation front is followed by a shock front. For handling such a problem, the Lax method can be used to smooth flow discontinuities through the differencing scheme, which implicitly introduces an artificial viscosity into the equations of motion.[10] Lax's scheme requires all gasdynamic equations to be expressed in Lagrangian form, in which the coordinates and state variables of a flow particle are a function of time t and a parameter ξ. The respective equations of continuity, momentum, and energy can be written as,

$$\frac{\partial}{\partial t}\left\{\frac{\rho(\xi,0)}{\rho(\xi,t)}\right\}=\frac{\partial u}{\partial \xi} \quad (9)$$

$$\frac{\partial u}{\partial t}=-\frac{1}{\rho(\xi,0)}\frac{\partial p}{\partial \xi} \quad (10)$$

$$\frac{\partial}{\partial t}\left(e+\frac{1}{2}u^2\right)=-\frac{1}{\rho(\xi,0)}\frac{\partial}{\partial x}(pu) \quad (11)$$

where ρ is the density of the mixture, p the pressure, e the specific internal energy, and u the velocity.

The equation of state of the mixture is given by

$$p=\left(\frac{1-\omega_0-g_s}{\mu_i}+\frac{\omega_0-g}{\mu_v}\right)\rho\Re T \quad (12)$$

where $\Re$ is the gas constant, g the condensate mass fraction, g_s the mass fraction of solid particles, ω_0 the initial specific humidity $(\rho_v+\rho_\ell')/\rho$, where ρ_v and ρ_ℓ' are the density of vapor and the mass of liquid phase per unit volume of mixture, and μ_i and μ_v are the molecular weights of inert carrier gas and vapor, respectively. The internal energy of the mixture is expressed as

$$e=\{(1-\omega_0-g_s)C_{pi}+\omega_0 C_{pv}+g_s h_s/T\}T-gL-p/\rho \quad (13)$$

where C_{pi} and C_{pv} are the specific heats at constant pressure of inert gas and vapor, respectively; h_s the specific enthalpy of solid particles; and L the latent heat of vaporization. The supersaturation is given by

$$s=\frac{p_v}{p_s}=\frac{p}{p_s}\frac{\omega_0-g}{(1-\omega_0-g_0)\dfrac{\mu_v}{\mu_i}+(\omega_0-g)} \quad (14)$$

where the saturation pressure for water vapor is

$$p_s=10^{(B-A/T)} \quad A=2263.0°\text{K}, \quad B=6.064 \quad (15)$$

The surface tension is assumed to vary linearly with temperature as[10]

$$\sigma = 128 - 0.192T \text{ (dyne/cm)} \qquad (16)$$

The other physical quantities are the same as those used in Ref. 1. Concerning the physical properties of solid particles, those of SiO_2 are used, although they have negligible effect on the overall properties of the mixture. Detailed data on contact angles in the system of solid particles of Aitken nuclei wetted by water are not available. The angles $\theta = 90°$ and 120° are taken as representative values. Although the values of the vibrational frequency of adsorbed atoms and the free energy of desorption are not certain, they are roughly estimated as $\nu = (0.1 \sim 10) \times 10^{13}$/sec and $\Delta G_d = (2 \sim 200) \times 10^3$ cal/g-atom,[7] that is, $R_H = 10^4 \sim 10^8$ cm and $\beta_d = 3 \sim 300$.

Equations (9)-(12) together with the rate equations (5-8) and the foregoing thermodynamic and physical properties describe the nonequilibrium heterogeneous condensation of water vapor in one-dimensional nonstationary flows. They can be solved numerically using the Lax method following the techniques of Ref. 10.

Numerical Results and Discussion

The numerical calculations were performed on an IBM 370-165 at the University of Toronto.[10] The following initial conditions were used: nitrogen-water vapor mixture of relative humidity of 97.3% and at 295.3°K in the driver section and air in the low-pressure chamber at 295.3°K and 100 mm Hg, giving a diaphragm-pressure ratio of 6.8.

The predicted flowfield of the nonequilibrium nonstationary rarefaction wave in the physical (x,t) plane is shown in Fig. 3, where the numerical constants of heterogeneous nucleation, $\theta = 90°$, $R_H = 0.3 \times 10^6$ cm, $\beta_d = 34$, and curve B in Fig. 1 were used. The head of the rarefaction wave moves onto the mixture at rest in the driver chamber with the state sound speed ($-x$ direction). Behind the rarefaction, the mixture is cooled to supersaturation. Consequently, nucleation takes place on the heterogeneous nuclei with an appropriate time lag. In Fig. 3, the condensation front is defined by the locus of points along particle paths where the supersaturation reaches its maximum values (as shown in Fig. 5). If the heat release associated with condensation causes the characteristics to intersect, then the condensation wave is followed by a shock wave,[1,10] defined by the locus of points of pressure maxima after supercooling. Between the condensation-wave front and the shock wave, there exists a condensation zone (hatched in the figure) where the flow variables change appreciably due to heat release. It can be seen from the figure that condensation in the heterogeneous case ($\theta = 90°$) occurs sooner than in the homogeneous case (HM). In addition, the width between two fronts is narrower for heterogeneous condensation with $\theta = 90°$.

Figures 4-6 show time-variations of the pressure, supersaturation and condensates mass fraction along particle paths initially at -5, -10, and -20 cm from the diaphragm of the shock tube. In heterogeneous condensation, the decrease in the pressure (Fig. 4) as well as the temperature before the onset of condensation is smaller than that in homogeneous condensation. The successive rise of their values after the onset of condensation is also smaller. Consequently, the onset

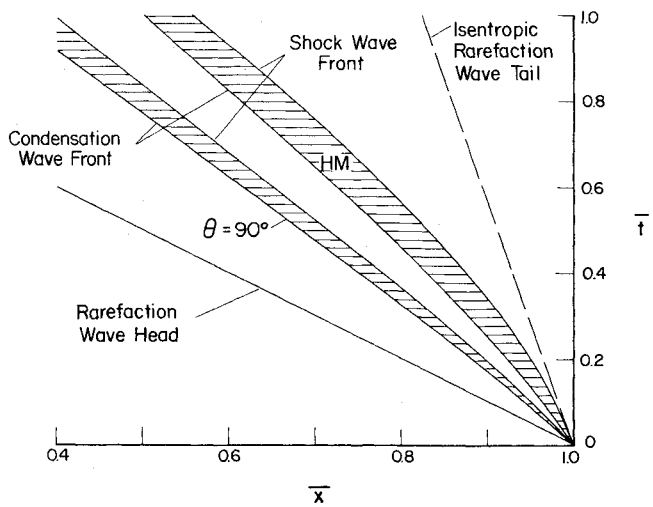

Fig. 3 Condensation wave structure.

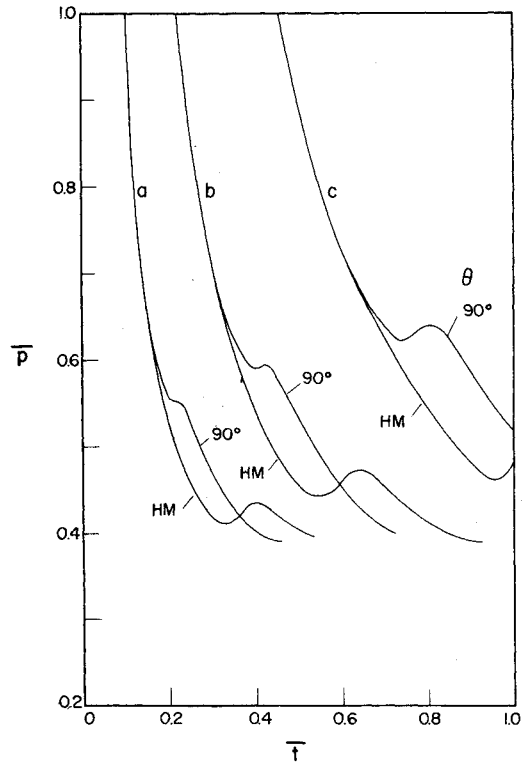

Fig. 4 Time variation of pressure along particle paths initially at −5 (a), −10 (b), −20 (c) cm from the diaphragm ($\bar{p} = p/680$ mm Hg, $\bar{t} = t/1.2$ msec).

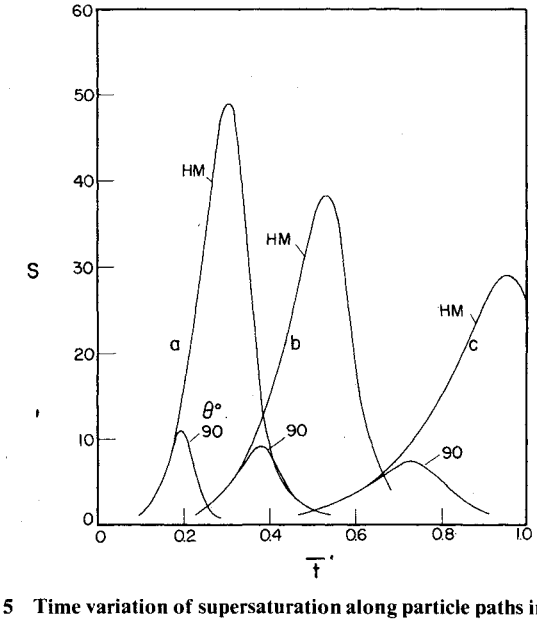

Fig. 5 Time variation of supersaturation along particle paths initially at −5 (a), −10 (b), −20 (c) cm from the diaphragm ($s = p_v/p_s$, $\bar{t} = t/1.2$ msec).

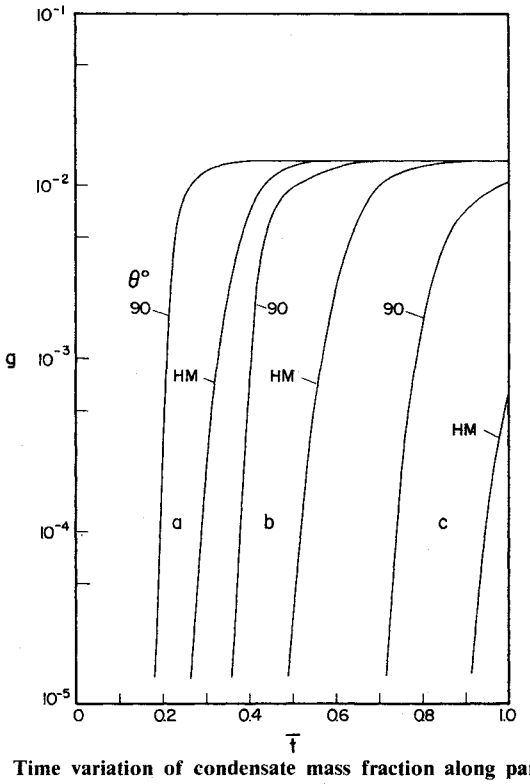

Fig. 6 Time variation of condensate mass fraction along particle paths initially at −5 (a), −10 (b), −20 (c) cm from the diaphragm ($\bar{t}=t/1.2$ msec).

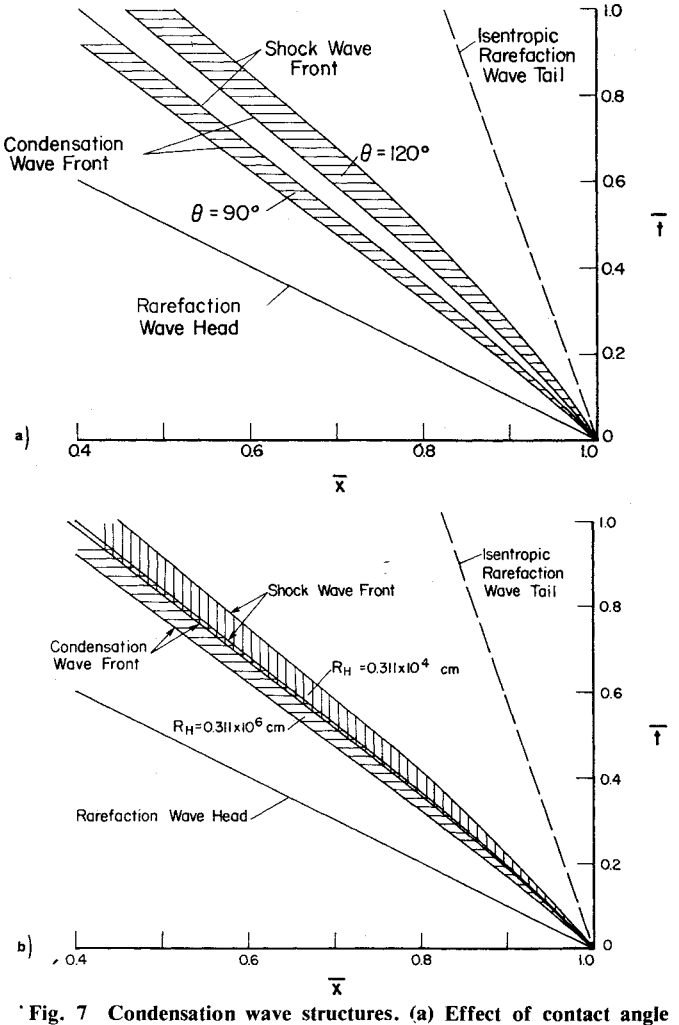

Fig. 7 Condensation wave structures. (a) Effect of contact angle $\theta(R_H=0.311\times10^6$ cm), (b) Effect of factor $R_H(\theta=90°)$.

of heterogeneous condensation occurs closer to the rarefaction-wave head (see Fig. 3), and from Fig. 5, it is readily seen that heterogeneous nucleation leads to lower values of maximum supersaturation. Figure 6 shows that in the heterogeneous case, the condensate mass fraction increases more sharply up to the equilibrium value than in the homogeneous case.

Since the supersaturation is directly related to the nucleation rate, the latter attains its maximum approximately at the highest supersaturation. Thereafter, the condensation of water vapor onto the solid nuclei plays an increasingly important role in the phase-changing process. The heat release due to condensation causes an increase in the temperature of the mixture. In heterogeneous nucleation, the activation energy of nucleation is greatly reduced by the difference of the interfacial energies between the liquid-vapor, solid-vapor, and solid-liquid interfaces, acting equivalently to decrease the surface tension of the liquid-vapor interface. Less activation energy results in a higher nucleation rate with lower supersaturation, lower super-cooling, a higher propagation velocity of the condensation wave, and a narrower condensation zone.

As mentioned before, the size distribution of condensation nuclei hardly affects the condensation process in the expansion of the mixture, unless their sizes are comparable to those of nucleating embryos. Other factors controlling heterogeneous nucleation are the concentration of adsorbed monomers on the surface of the substrate and the contact angles of embryos. The former is characterized by the vibrational frequency of adatoms $\nu(R_H)$ and the desorption free energy of adsorbed monomers $\Delta G_d(\beta_d)$. Since the activation energy of nucleation is much larger than the desorption energy of adsorbed monomers, the latter does not greatly affect the nucleation process but reduces slightly the overall activation energy of nucleation. The factor R_H has a physical meaning related to the concentration of monomers adsorbed onto the surface of the substrate. It is a constant coefficient of the nucleation rate n. In the expression of the condensate mass, it is always coupled with the size-distribution function of heterogeneous nuclei. The factor R_H therefore means the influence of the overall number of nuclei or the overall surface area of nuclei.

Figure 7 shows the effect of both the contact angle $\theta=90°$, 120° and the factor $R_H=0.311\times10^6$, 0.311×10^4 cm. For larger contact angles (Fig. 7a), which means embryos of more

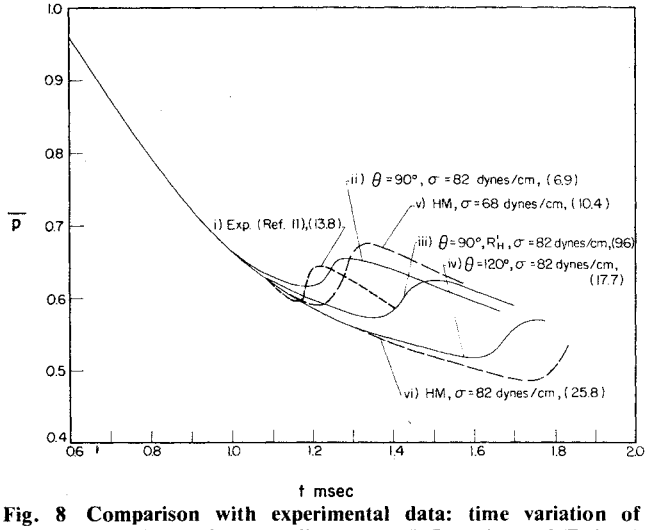

Fig. 8 Comparison with experimental data: time variation of pressure at −23.4 cm from the diaphragm. (i) Experimental (Ref. 11) $s_{onset}=13.8$. (ii) Heterogeneous, $\theta=90°$, $R_H=3.11\times10^6$ cm, $\sigma=82$ dyne/cm, $s_{onset}=6.9$. (iii) Heterogeneous, $\theta=90°$, $R_H=3.11\times10^4$ cm, $\sigma=82$ dyne/cm, $s_{onset}=9.6$ (iv) Heterogeneous, $\theta=120°$, $R_H=3.11\times10^6$ cm, $\sigma=82$ dyne/cm, $s_{onset}=17.7$ (v) Homogeneous, $\sigma=68$ dyne/cm, $s_{onset}=10.4$ (vi) Homogeneous, $\sigma=82$ dyne/cm, $s_{onset}=25.8$.

spherical shape, the heterogeneous nucleation loses its influence and tends to have the features of homogeneous nucleation. Reducing the value of the factor R_H (Fig. 7b), leads to a lower nucleation rate and higher supercooling. It should be noted that the factor R_H of two orders less in its value has an influence less than that of $\theta = 120°$. The contact angle is the most significant feature of heterogeneous condensation. Consequently, for an accurate prediction of such flowfields, the contact angle of embryos nucleating on the substrate of solid particles must be estimated carefully. Yet, other parameters, including the size distribution of heterogeneous nuclei can be estimated roughly without serious effects.

The numerical results can be compared with experimental data from Ref. 11. Following the same considerations of the pressure history discussed in Ref. 1, the space location of the experimental measurement, $x = -17.0$ cm from the diaphragm, was selected as corresponding to $x = -23.4$ cm. To obtain a reasonable fit with the experimental data, in Ref. 1, the surface tension was changed from the semiempirical expression (16), $\sigma = 82$ dyne/cm to 68 dyne/cm, with the conclusion that choosing a suitable value for the surface tension can provide a good fit to the experimental results. As shown in Fig. 8, in heterogeneous condensation, a similar fit can be obtained by replacing the surface tension by the contact angle. By choosing a suitable value for the contact angle ($\theta = 90°$), the experimental data can be fitted fairly well except for the supersaturation at the onset of condensation. Concerning the relation between the supercooling and the cooling rate, the best-fit conditions for the pressure history, $\theta = 90°$ in the heterogeneous case and $\sigma = 68$ dyne/cm in the homogeneous case, result in the poorest agreement.[9] These best fits also give points very close to each other on the time-distance plot shown in Fig. 7 of Ref. 1. Consequently, the schlieren records of Ref. 12 cannot be used as a decisive test for the two competing theories, since the trajectory of the condensation shock agrees with either of the two theories. The relative importance of both processes depends greatly on the cooling rate. Higher cooling rates ($\gtrsim 1°C/\mu sec$) may be favorable for homogeneous nucleation and condensation. Values of the cooling rates in the present case were $0.1 \sim 0.2°C/\mu sec$,[9] and did not provide a decisive criterion.

An inspection of Fig. 8 shows that the experimental time-variation of pressure at the onset of condensation is extremely sharp compared with the numerical results. This is not surprising in view that the implicit artificial viscosity used in the numerical analysis tends to spread the condensation and shock fronts. It is also worth noting that factors such as coagulation, solubility, or electrical charges have not been treated in the present study. When nuclei or embryos have a higher number density,coagulation is another factor to be considered. By assuming the coagulation constant as 10^{-9} cm^3/(sec particles)[13] and the characteristic time as 10^{-3} sec, the number density above which coagulation has a considerable effect can be estimated as 10^{12} particles/cm^3. Since the assumed number density of heterogeneous nuclei was about 10^5 particles/cm^3, coagulation would hardly affect the results within such a characteristic time. In the homogeneous nucleation case, however, it may be a factor to be taken into account because of the higher number density of nucleated droplets ($>10^{15}$ particles/cm^3). We do not have enough physical data on the effects of solubility and chemical and electrical activities; however, they are expected to have appreciable effects for real aerosols. Additional experimental data, analytical results, and useful discussions may be found in Ref. 14.

Conclusions

By using a macroscopic model of heterogeneous nucleation, an analytical study was made of the condensation of water-vapor/carrier-gas mixtures in a nonequilibrium nonstationary rarefaction wave generated in a shock tube. Nucleation is assumed to take place heterogeneously on idealized smooth, spherical solid particles of Aitken nuclei, which are chemically and electrically inert.

In the process of heterogeneous nucleation, the controlling factors are the size distribution of nuclei, the concentration of monomers adsorbed on the surface of the substrate, and the contact angle of embryos. Of these factors, the dominant one is the contact angle. By decreasing the contact angle, the activation energy of nucleation is greatly reduced, and the onset of condensation occurs closer to the rarefaction-wave head where temperatures and pressures are higher and at less supercooled states and lower supersaturations.

When nuclei are in the size range of one or two orders larger than that of the embryos ($R \sim 10^{-5}$ cm) and the value of the contact angle is not too large ($\theta < 120°$), heterogeneous nucleation dominates the condensation process and homogeneous nucleation can be neglected. For nuclei under such conditions, the size distribution and concentration of monomers adsorbed on the surface of the nuclei are not significant factors in the overall process of heterogeneous condensation.

An appropriate value for the contact angle makes it possible to fit the numerical results with available experimental data. From such a fit, a contact angle of 90° appears reasonable, although this cannot substitute for actual measurements. The experimental results can be explained equally well by either a homogeneous or a heterogeneous nucleation theory with suitable values of surface tension and contact angle, respectively. In view that the former requires a lower value of surface tension and a possible consideration of coagulation, heterogeneous nucleation and condensation might be a physically more acceptable model to fit the experiments. However, a decisive experiment would be very valuable and would confirm which of the two models, heterogeneous or homogeneous nucleation, describes the physical situation. Perhaps both might go on simultaneously, unless great care was taken to isolate one of them.

The shape of embryo and substrate different from a sphere, chemical or electrical activity, and the solubility of nuclei were not taken into account and these could be important in real aerosol systems. However, the present study can be readily extended to examine the effects of such factors if the physical data were provided. Furthermore, the analysis lends itself to simultaneous applications of homogeneous and heterogeneous nucleation and to other problems of heterogeneously phase-changing processes.

Acknowledgments

The financial support received from the National Research Council of Canada, the Atomic Energy of Canada Ltd. (Chalk River), and the U.S. Air Force Office of Scientific Research (AF-AFOSR 72-2274) is acknowledged with thanks.

References

[1]Sislian, J.P. and Glass, I.I., "Condensation of Water Vapor in Rarefaction Waves-I. Homogeneous Nucleation," *AIAA Journal*, Vol. 14, Dec. 1976, pp. 1731-1737.

[2]Turnbull, D., *Progress in Solid State Physics*, Academic Press, New York, 1965.

[3]Hirth, J. P. and Pound, G. M., *Condensation and Evaporation*, Pergamon Press, Oxford, 1963.

[4]Fletcher, H. N., *The Physics of Rain Clouds*, Cambridge University Press, Cambridge, 1962.

[5]Junge, C., "Gesetzmässigkeiten in der Grössenverteilung Atmosphärischer Aerosole über dem Kontinent," *Deutscher Wetterdienst in der U.S. Zone*, Vol. 5, 1952, pp. 261-277.

[6]Sigsbee, R. A., "Vapor to Condensed-Phase Heterogeneous Nucleation," in *Nucleation*, Ed., A. C. Zettlemoyer, Marcel Dekker, New York, 1969, chapt. 4, pp. 151-224.

[7]Pound, G. M., Simnad, M. T., and Yang, L., "Heterogeneous Nucleation of Crystals from Vapor," *Journal of Chemical Physics*, Vol. 22, July 1954, pp. 1215-1219.

[8]Fletcher, N. H., "Size Effect in Heterogeneous Nucleation," *Journal of Chemical Physics*, Vol. 29, Sept. 1958, pp. 572-576.

[9]Kotake, S. and Glass, I. I., "Condensation of Water Vapour on Heterogeneous Nuclei in a Shock Tube," University of Toronto Institute for Aerospace Studies, Toronto, Canada, UTIAS Rept. 207, April 1976.

[10]Sislian, J. P., "Condensation of Water Vapour with or without a Carrier Gas in a Shock Tube," University of Toronto Institute for Aerospace Studies, Toronto, Canada, UTIAS Rept. 201, Nov. 1975.

[11]Kalra, S. P., "Experiments on Nonequilibrium, Nonstationary Expansion of Water Vapour/Carrier Gas Mixture in a Shock Tube," UTIAS Rept. 195, April 1975; see also Ref. 14.

[12]Glass, I. I. and Patterson, G. N., "A Theoretical and Experimental Study of Shock-Tube Flows," *Journal of the Aeronautical Sciences*, Vol. 22, Feb. 1955, pp. 73-100.

[13]Green, H. L. and Lane, W. R., *"Particulate Clouds,"* E&F.N. Spoon Ltd., London, 1964.

[14]Glass, I.I., Kalra, S.P., and Sislian, J.P., "Condensation of Water Vapor in Rarefaction Waves-III. Experimental Results," submitted to *AIAA Journal* for publication.